ORGANOMETALLICS

pubs.acs.org/Organometallics Article

# Insertions of Isocyanides in Diamidoamine Rhenium(III) Complexes

Liana Pauly, Abdullahi K. Adegboyega, Caleb A. Brown, Damaris E. Pérez, and Elon A. Ison*

Cite This: *Organometallics* 2024, 43, 3002−3012 Read Online

ACCESS | Metrics & More | Article Recommendations | Supporting Information

**ABSTRACT:** Rhenium(III) complexes of the form (CO)Re(DAAm) (R) **1** (DAAm = $N^1$-mesityl-$N^2$-(2-(mesitylamino)-ethyl)-$N^2$-methylethane-1,2-diamine) (*R* = benzyl, **1a**; methyl, **1b**; 4-OMe-benzyl, **1c**) react with isocyanides R′NC, (R′ = 2,6-dimethylphenyl, *tert*-butyl) to give $\eta^1$ and $\eta^2$ iminoacyl complexes. When 2,6-dimethylphenylisocyanide reacts with **1a**, the resulting iminoacyl complex was $\eta^2$ while the reaction with **1c** leads to an $\eta^1$ iminoacyl complex. However, the less bulky isocyanide *tert*-butyl isocyanide produced only $\eta^2$ iminoacyl complexes with **1b** and **1c**. Carbene complexes were obtained by the reaction with methyl triflate. The mechanism for the formation of the iminoacyl complexes in this study was also investigated by DFT (APFD).

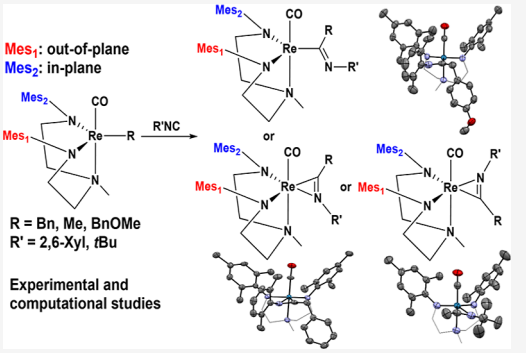




## INTRODUCTION

Isocyanides are a class of organic molecules that have the C≡N functional group. Over the years, the scientific community has found some important applications for this class of molecule, such as multicomponent reactions, the synthesis of various heterocycles, cycloadditions, transition-metal insertions, and the generation of acyclic and heterocyclic aminocarbenes.[1−16]

In reactions with metal complexes, carbon monoxide has been more studied than isocyanides, despite the versatility of the latter.[6] Like CO, the lone pair on the carbon atom of isocyanides can coordinate to transition metals.[11] However, compared to CO, isocyanides have weaker $\pi$-acceptor and stronger $\sigma$-donor properties.[6] One important advantage of isocyanides over carbon monoxide is the presence of R substituents on the N atoms, which makes these organic molecules sterically and electronically tunable.[1,6,15,17] For example, isocyanides become better $\pi$-acceptors when the substituent is an aromatic group, due to the delocalization of electron density into the aromatic ring.[11]

Insertions of small molecules such as carbon monoxide and isocyanides into metal−carbon bonds are fundamentally important reactions for the formation of new C−C bonds.[15,18−20] For group 4, the mechanistic and stereochemical aspects of CO insertion have been extensively studied. For example, Floriani reported that the O atom was positioned between the alkyl ligands in $(Cp)_2Zr(R)_2$, adopting an "O inside" configuration (Scheme 1a).[21] Similar behavior was observed by Erker and Rosenfeldt.[22−25] However, some computational work performed by Lauher and Hoffmann suggested that the most stable product should have the O atom away from the two alkyl ligands, as an "outside" isomer (Scheme 1a).[26] Erker and Rosenfeldt showed experimentally that the carbonylation reaction afforded the "O−outside" isomer at −78 °C as the kinetic product, while the thermodynamic product, the "O−inside" isomer, was obtained at temperatures higher than −60 °C (Scheme 1a).[22]

Recently, Norton reported a similar insertion reaction with *tert*-butyl isocyanide into one of the zirconium−methyl bonds of $Cp^*_2Zr(CH_3)_2$. This reaction afforded the monoinsertion product $Cp^*_2Zr(iminoacyl)CH_3$, with the "N−outside" configuration, which converts entirely to the "N-inside" isomer at 80 °C (Scheme 1b).[27] The cleavage of the methyl ligand by treating the iminoacyl complex with the Brønsted acid $CpCr(CO)_3H$ is proposed to result from the initial protonation of the nitrogen in the iminoacyl ligand, followed by subsequent outside-to-inside rotation and eventual transfer of the proton onto the Zr−C bond.[27] These studies suggest that the stereochemical outcomes of insertion reactions can have a significant effect on reactivity.

In recent years, our group has shown that the insertion of CO and isocyanides into Re−R bonds, followed by treatment with an electrophile, results in rare examples of Re(III) and Re(V) Fischer carbenes.[28] The reactions with isocyanide proceed by insertion of the isocyanide substrate into a Re−Me bond to form iminoacyl complexes. These iminoacyl complexes were not isolated, but were identified by $^1$H NMR spectroscopy and then converted quantitatively to Fisher carbenes. In this article, we explore in detail, experimentally,

Received: July 29, 2024
Revised: November 9, 2024
Accepted: November 14, 2024
Published: November 26, 2024






https://doi.org/10.1021/acs.organomet.4c00338
*Organometallics* 2024, 43, 3002−3012

**Scheme 1. Comparison of Isocyanide Insertion Reactions Reported Previously with the Work Presented in This Study**

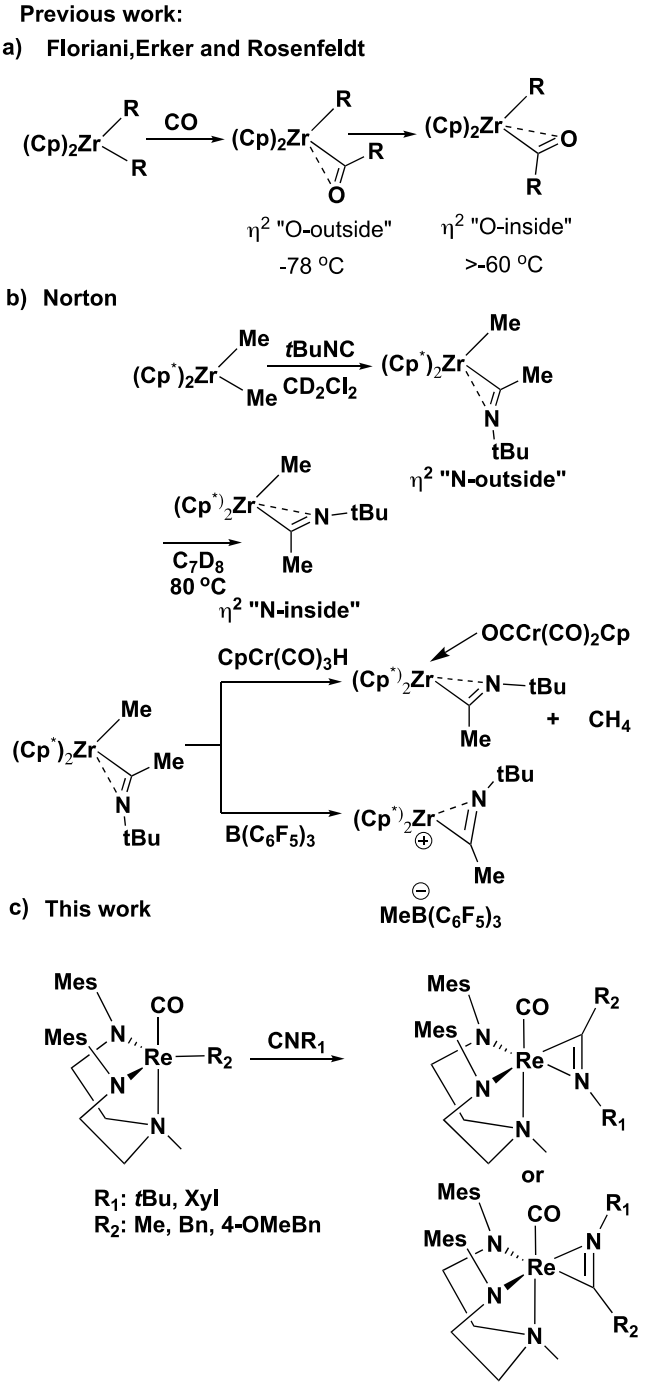


and with DFT studies, the insertion of isocyanides into Re−R (R = Me, benzyl) bonds to form rhenium(III) iminoacyl and carbene complexes. The iminoacyl complexes obtained differ in the position of the imino N atom depending on the steric properties provided by the substituent on the isocyanide substrate (Scheme 1c). In addition, insertion reactions result in $\eta^1$ or $\eta^2$ iminoacyl complexes depending on the nature of the isocyanide substituent and the alkyl or benzyl group attached to rhenium.[1] This is significant because experimental and theoretical studies suggest that $\eta^1$-coordination is usually favored by late transition metals, whereas early transition metals have a tendency for binding in an $\eta^2$-coordination mode.[1] The observation of both hapticities for complexes with the same metal and ligand set is quite rare.

## RESULTS AND DISCUSSION

**Synthesis of Re(III) Complexes.** Re(III) complexes of the form (CO)Re(DAAm) (R) **1** (DAAm = $N^1$-Mesityl-$N^2$-(2-(mesitylamino)-ethyl)-$N^2$-methylethane-1,2-diamine) (*R* = benzyl, **1a**; methyl, **1b**; 4-methoxybenzyl, **1c**) were utilized. The synthesis of **1b** was previously described by our group resulting from the reaction of (CO)Re(DAAm)(OAc) with MeMgCl.[28] Complexes **1a** and **1c** were similarly synthesized with the appropriate Grignard reagents, benzyl magnesium chloride and 4-methoxybenzyl magnesium chloride, respectively. The X-ray crystal structure of **1a**, shown in Figure 1, confirms the expected connectivity. Similarly, **1c** was confirmed by NMR spectroscopy as well as X-ray crystallography (see the Supporting Information).

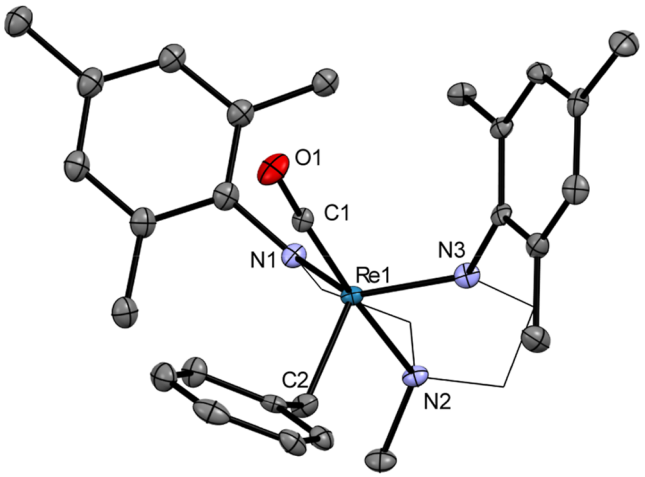


**Figure 1.** X-ray crystal structure of **1a**. Ellipsoids are at 50% probability level. Hydrogen atoms were omitted, and the ligand is displayed in wireframe for clarity. Selected bond lengths (Å) and angles (deg): Re1−C1, 1.856(5); Re1−N1, 1.945(5); Re1−N2, 2.252(5); Re1−N3, 1.917(4); Re1−C2, 2.127(6); O1−C1, 1.174(7); C1−Re1−N1, 96.2(2); C1−Re1−N3, 97.6(2); N1−Re1−N3, 127.3(2); C1−Re1−C2, 95.2(2); N1−Re1−C2, 117.9(2); N3−Re1−C2, 111.1(2); C1−Re1−N2, 174.2(2); N1−Re1−N2, 80.3(2); N3−Re1−N2, 81.1(2); C2−Re1−N2, 90.5(2).

**Synthesis of Iminoacyl Rhenium(III) Complexes.** The reaction of complexes (CO)Re(DAAm) (*R*) **1** (*R* = benzyl, **1a**; methyl, **1b**; 4-methoxybenzyl, **1c**) with the isocyanides R′NC, (R′ = 2,6-dimethylphenyl, *t*ert-butyl) at room temperature affords $\eta^2$-iminoacyl complexes **2a**, **2b**, **2c**, or the $\eta^1$-iminoacyl, **2d** (Scheme 2). The ancillary mesityl rings differed in their position as $Mes_1$ was in plane defined by the CO ligand, the rhenium atom, and the N(Me) group while $Mes_2$ was orthogonal to this plane. The xylyl group was consistently on the same side as $Mes_1$ while the *tert*-butyl group was on the same side as $Mes_2$. The connectivity of these novel iminoacyl complexes was confirmed by X-ray crystallography and is depicted in Figures 2−5. Complexes **1** (**a**-**c**) have a plane of symmetry; therefore, they cannot produce optical isomers. However, the reactions with the isocyanides listed above afforded conformational isomers that were observed in each unit cell. For example, Figure 6 shows the unit cell of **2a** with the two conformational isomers, where the position of the


https://doi.org/10.1021/acs.organomet.4c00338
Organometallics 2024, 43, 3002−3012

**Scheme 2. Synthesis of Iminoacyl Rhenium(III) Complexes from 1. These Reactions Were Performed in Dichloromethane at 25 °C with One Equivalent of Isocyanide**

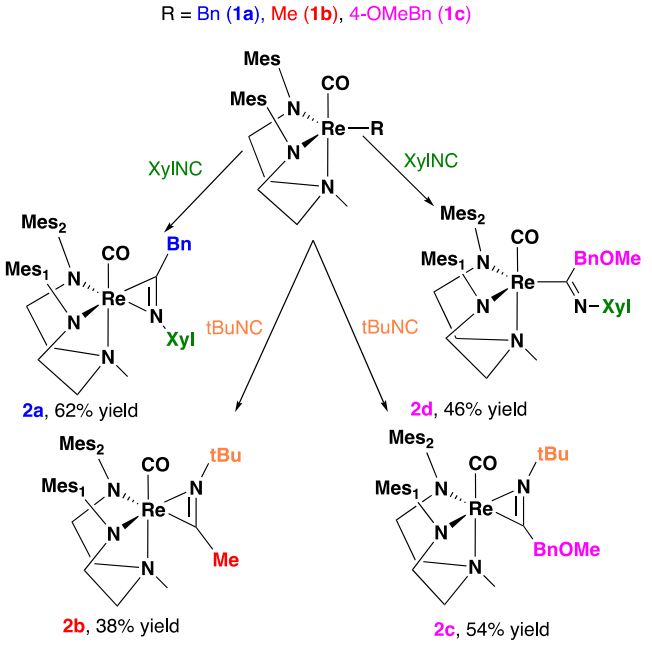


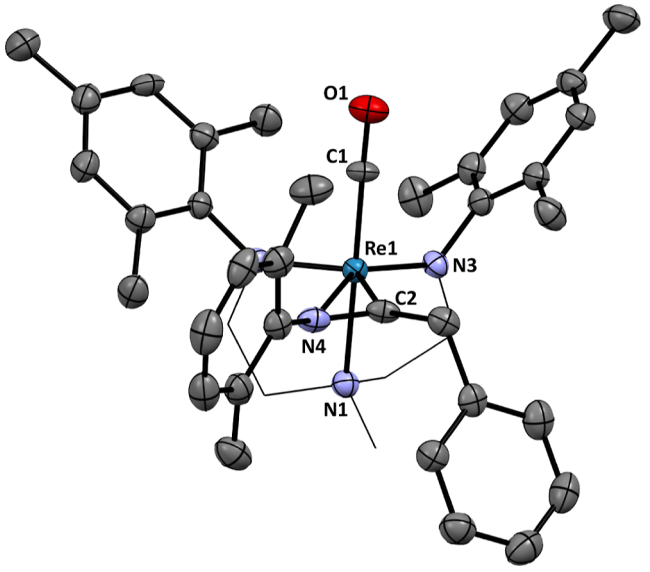


**Figure 2.** X-ray crystal structure of **2a**. Ellipsoids are at a 50% probability level. Hydrogen atoms and the cocrystallized solvent were omitted, and the ligand is displayed in wireframe for clarity. Selected bond lengths (Å) and angles (deg): Re1−N1, 2.265(4); Re1−N2, 1.981(4); Re1−N3, 1.929(4); Re1−N4, 2.370(4); Re1−C1, 1.867(5); Re1−C2, 2.058(5); C2−N4, 1.279(8); O1−C1, 1.167(6); N1−Re1−N4, 89.59(15); N2−Re1−N1, 80.60(15); N2−Re1−N4, 95.77(17); N3−Re1−N1, 80.43(17); N3−Re1−N2, 114.34(18); N3−Re1−N4, 145.89(17); O1−C1−Re1, 176.6(5).

imino nitrogen atom in relation to the Re−CO bond changes. To accommodate the size of the xylyl group, the mesityl ligand was rotated, with the in-plane mesityl, $Mes_1$, on the same side of the bulky R group of the isocyanide.

As depicted in Scheme 2, isocyanide insertions were also investigated with other rhenium complexes. Treatment of *tert*-butyl isocyanide with **1b** at room temperature results in the formation of **2b**. Unlike **2a**, the X-ray crystal structure of **2b** shows the imino N atom on the same side as the out-of-plane mesityl group, $Mes_2$ (Figure 3). This suggests that the *tert*-butyl group is less sterically encumbered compared to the xylyl group in **2a**. To examine this further, we investigated the reaction of *tert*-butyl isocyanide with benzyl complex **1c**. This

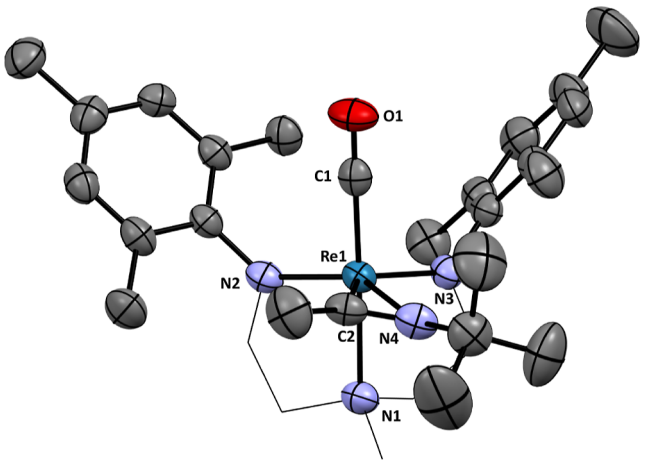


**Figure 3.** X-ray crystal structure of **2b**. Ellipsoids are at a 50% probability level. Hydrogen atoms and the cocrystallized solvent were omitted, and the ligand is displayed in wireframe for clarity. Selected bond lengths (Å) and angles (deg): Re1−N1, 2.285(4); Re1−N2, 1.922(4); Re1−N3, 1.999(3); Re1−N4, 2.312(4); Re1−C1, 2.285(4); Re1−C2, 2.048(4); C2−N4, 1.264(6); O1−C1, 1.168(5); N1−Re1−N4, 87.20(14); N2−Re1−N1, 81.01(15); N2−Re1−N3, 112.58(14); N2−Re1−N4, 141.71(15); N1−Re1−C2, 111.18(18); C1−Re1−N1, 176.90(16); O1−C1−Re1, 175.5(5).

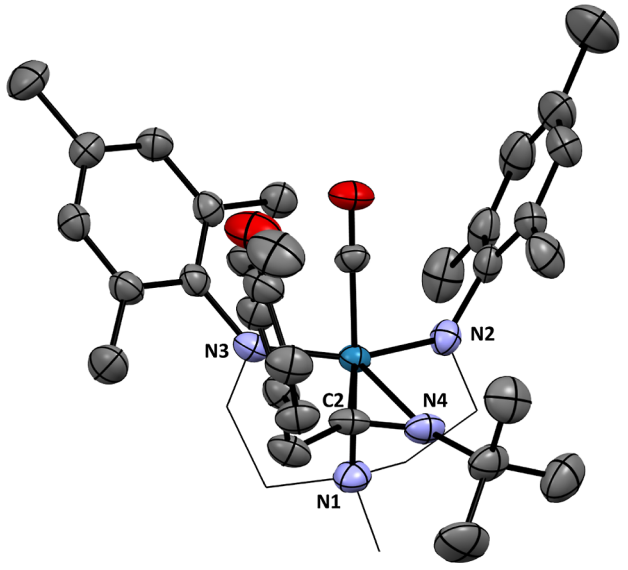


**Figure 4.** X-ray crystal structure of **2c**. Ellipsoids are at a 50% probability level. Hydrogen atoms and the cocrystallized solvent were omitted, and the ligand is displayed in wireframe for clarity. Selected bond lengths (Å) and angles (deg): Re1−C1, 1.857(4); Re1−N1, 2.281(3); Re1−N2, 1.992(3); Re1−N3, 1.925(3); Re1−N4, 2.310(3); Re1−C2, 2.057(4); O1−C1, 1.173(5); N4−C2, 1.256(5); N2−Re1−N1, 80.58(13); N2−Re1−N4, 98.77(13); N3−Re1−N2, 112.43(13); N3−Re1−N1, 80.96(13); N3−Re1−N4, 143.75(13); N3−Re1−C2, 113.02(15); N1−Re1−N4, 86.67(12); C1−Re1−N1, 175.25(14); O1−C1−Re1, 179.4(4).


https://doi.org/10.1021/acs.organomet.4c00338
Organometallics 2024, 43, 3002−3012

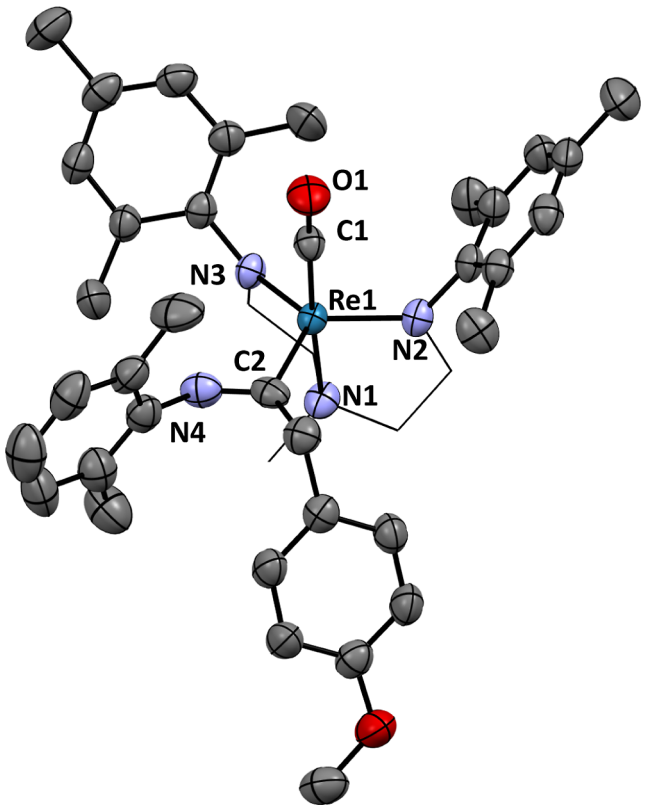


**Figure 5.** X-ray crystal structure of **2d**. Ellipsoids are at a 50% probability level. Hydrogen atoms and the cocrystallized solvent were omitted, and the ligand is displayed in wireframe for clarity. Selected bond lengths (Å) and angles (deg): Re1−C1, 1.865(3); Re1−N1, 2.235(2); Re1−N2, 1.997(2); Re1−N3, 1.954(2); Re1−C2, 2.080(2); O1−C1, 1.168(4); N4−C2, 1.283(4); N2−Re1−N1, 80.75(10); N3−Re1−N2, 119.19(10); N3−Re1−N1, 80.23(10); N3−Re1−C2, 122.10(12); N2−Re1−C2, 116.75(12); C1−Re1−N1, 173.92(12); O1−C1−Re1, 178.7(3).

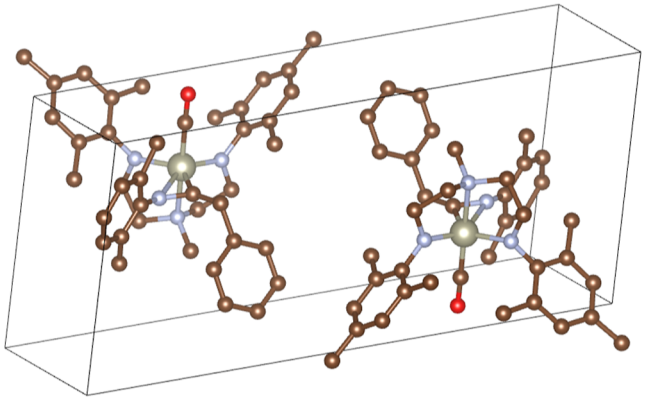

**Figure 6.** Unit cell of **2a** showing the two conformational isomers. Hydrogen atoms, cocrystallized solvent, and repeating molecules were omitted for clarity.

reaction afforded complex **2c** (Figure 4). When **1c** was treated with 2,6-dimethylphenylisocyanide, the iminoacyl complex, **2d**, was afforded (Figure 5). Unlike the previous complexes, however, **2d** features an $\eta^1$ iminoacyl ligand. Further, in contrast to **2a**, the imino N atom is on the same side as the out-of-plane mesityl group, $Mes_2$ in **2c**. Thus, the *tert*-butyl group is consistently on the same side as $Mes_2$, while the xylyl group is consistently on the same side as $Mes_1$. It should be noted that the methyl substituents in the 2,6-position of the xylyl group would be oriented directly into the plane defined by the CO ligand, the rhenium atom, and the N(Me) group as described above. In contrast, the *tert*-butyl group is oriented away from this plane. As a result, complexes with a *tert*-butyl substituent on the imino nitrogen are less sterically hindered than complexes with a xylyl group on the imino nitrogen. This hypothesis was confirmed when the steric maps for **2c** and **2d** were compared (see the Supporting Information).

The reason for the preference for $\eta^1$ or $\eta^2$ binding modes in iminoacyl ligands is not clear and does not appear to be well understood in the current literature. Although rhenium has been a particularly suitable metal to study the coordination chemistry of isocyanides due to the many stable and easily accessible oxidation states[29] available to this atom, insertion of isocyanides does not seem to be frequently investigated.[1] Alexander and co-workers reported two $\eta^1$ rhenium iminoacyl complexes that were achieved by insertion reactions into Re−C bonds.[20] In 1980 and 1982, Mays and co-workers reported two different studies with hydride rhenium dimers where upon treatment with isocyanides, those substrates were inserted into the rhenium-hydride bonds and the final products contained both $\eta^1$ and $\eta^2$ binding modes.[30,31] In both cases, the $\eta^1$ complexes featured imine nitrogens coordinated to two metal centers, and the $\eta^2$ complexes featured nitrogen and the carbon imine atoms each coordinated to a different metal center.[30,31]

It is also possible to find reports of other metals. For example, the triangular osmium cluster reported by Adams and Golembeski afforded isocyanide inserted products with both $\eta^1$ and $\eta^2$ conformations.[32] In the case of the latter, in one of the structures, both carbon and nitrogen are bound to different osmium atoms, while in the other structure, the carbon and nitrogen atoms are coordinated to only one osmium atom each.[32] The $\eta^1$ complex featured the carbon imine atom coordinated to two of the three metal centers.[32] The same type of coordination occurred in the clusters of cobalt and tungsten.[33,34].

Whitby and Davis reported in 1992 a zirconium complex that reacts with phenyl isocyanide to form an $\eta^1$ iminoacyl complex that rearranges to an $\eta^2$ binding mode upon warming to 40 °C.[35] Adams and Chodosh reported $\eta^1$ and $\eta^2$ iminoacyl molybdenum complexes, but in this case, the six-coordinate $\eta^1$ iminoacyl complex was coordinatively and electronically saturated, which precluded formation of the $\eta^2$ binding mode. The $\eta^2$ binding mode was realized in a five-coordinate version of the molecule that lacks an additional phosphite ligand. Thus, the binding mode of the iminoacyl ligand in this example is a function of the coordination environment at the metal center, with the higher hapticity occurring in the complex with the lower coordination number as expected.[36] However, in the case of **1a** and **1c**, the hapticity preference appears to be a function of the electronics at the metal complex.

To summarize, isocyanides readily insert into Re−R bonds to afford both $\eta^2$ and $\eta^1$ iminoacyl complexes. Both the stereochemistry and the hapticity of the iminoacyl ligand are influenced by the sterics and electronics of the substituent on the isocyanide substrate and the alkyl or benzyl ligand in the rhenium complex.

The $^{13}C$ NMR spectra for all iminoacyl complexes (224−234 ppm) are consistent with previous complexes that feature similar ligands.[37] For example, Norton and co-workers


https://doi.org/10.1021/acs.organomet.4c00338
Organometallics 2024, 43, 3002−3012

reported a zirconium $\eta^2$ iminoacyl complex with a $^{13}C$ NMR signal at $\delta$ 237 ppm.[27] This downfield shift is also observed in other zirconium complexes, such as ZrCp(ArO) ($\eta^2$-C-($CH_2$Ph)N-*t*-Bu) ($CH_2$Ph)] (ArO)2,3,5,6-$Ph_4C_6HO$; 4,6 *t*-$Bu_2$-2-$PhC_6H_2O$) ($\delta$ 242−244 ppm),[38] and [Zr{($^i$PrNH)C-($N^iPr)_2$}$_2$($CH_2$Ph){C($CH_2$Ph)N(2,6-$Me_2$Ph)}] ($\delta$ 253 ppm).[39] Similarly, Martins and co-workers reported the $^{13}C$ NMR chemical shift of the iminoacyl ligand at $\delta$ 241 ppm.[40] The zirconium iminoacyl complexes of Rothwell were reported to have their carbon atoms resonate between $\delta$ 235 and 250 ppm,[41] while Teuben and co-workers reported a titanium $\eta^2$ iminoacyl complex with the iminoacyl carbon resonance of about $\delta$ 215−230 ppm.[42] The isocyanide insertion of *m*-xylyl isocyanide into a tantalum hydride bond reported by Rothwell and co-workers also afforded a downfield $^{13}C$ NMR resonance at $\delta$ 240 ppm.[43] The cyclometalated tantalum iminoacyl species had a similar value at $\delta$ 243 ppm.[44] The reported $^{13}C$ chemical shift for the tungsten complex Cp*W(NO)($CH_2SiMe_3$)($\eta^2$-$CH_3CHCHCH_2C$ = $NC_6H_3Me_2$) occurs at $\delta$ 215 ppm.[45]

In another study of the synthesis and characterization of group 4−5 $\eta^2$ iminoacyl complexes, the $^{13}C$ NMR chemical shifts of the iminoacyl carbons were reported between $\delta$ 231 and 257 ppm.[46] The insertion of *tert*-butyl isocyanide and *m*-xylyl isocyanide into a niobium-phenyl bond yielded complexes with iminoacyl carbons at $\delta$ 219 and 230 ppm, respectively.[47] The niobium iminoacyl complex reported by Arnold and Bergman, however, was reported at $\delta$ 170 ppm.[48] However, the $\eta^2$ molybdenum iminoacyl complex reported by Otsuka and co-workers also had observed shifts at $\delta$ 196−198 ppm.[49] The reaction of aryl isocyanides with scandium complexes reported by Mindiola and co-workers afforded complexes with iminoacyl carbons at $\delta$ 259 ppm.[50] Finally, the $\eta^1$ iminoacyl complexes of rhenium were reported with $^{13}C$ shifts at $\delta$ 240 and 241 ppm.[20] Adams and co-workers reported $\eta^1$ and $\eta^2$ iminoacyl molybdenum chemical shifts for the iminoacyl carbon at $\delta$ 155 ppm for the former, while the chemical shifts for the latter complexes were reported at $\delta$ 195 and 197 ppm complexes.[36]

In contrast, the iminoacyl carbons of late transition metals seem to be observed upfield and commonly assume an $\eta^1$ coordination mode.[1] For example, Vicente and co-workers reported the product of the insertion reaction of 2,6-dimethylphenyl isocyanide into a palladium−carbon bond at $\delta$ 181 ppm.[51] In another study, the same group reported the carbon of iminoacyl palladium complexes at $\delta$ 171−178 ppm.[52] However, the reaction of a copper hydride dimer with benzyl isocyanide afforded an $\eta^1$-formimidoyl complex with $^{13}C$ NMR at $\delta$ 210 ppm.[53] The nickel iminoacyl complexes of Figueroa and co-workers was observed at $\delta$ 156 and 157 ppm.[54] Thus, chemical shifts for **2a**−**2d** are more consistent with electron-deficient early transition-metal complexes than corresponding late transition-metal complexes. IR spectra for the complexes of this present study are consistent with their assignment as iminoacyl complexes, as **2a**, **2b**, and **2d** display ATR-FTIR signals at 1600, 1616, and 1684 $cm^{-1}$, respectively. These signals are consistent with the iminoacyl complexes of the Norton[27] and Alexander[20] groups who reported signals at 1610 and 1611 $cm^{-1}$, respectively. Other early and late transition-metal $\eta^1$ and $\eta^2$ iminoacyls are also reported in this range.[41,42,46,49,51,52,54−57]

**Synthesis of Re(III) Carbenes.** We previously reported that the treatment of acyl and iminoacyl complexes (generated in situ) with Brønsted and Lewis acids results in the formation of Fisher carbene complexes.[28] Similarly, when **2a** was treated with one equivalent of methyl triflate, and when **1c** was treated with one equivalent of *m*-xylyl isocyanide followed by one equivalent of methyl triflate, the cationic rhenium carbene complexes **3** and **4** (Scheme 3) were afforded. These

**Scheme 3. Reaction of 2a′ with Methyl Triflate and 1c with 2,6-Dimethylphenyl Isocyanide and Methyl Triflate**

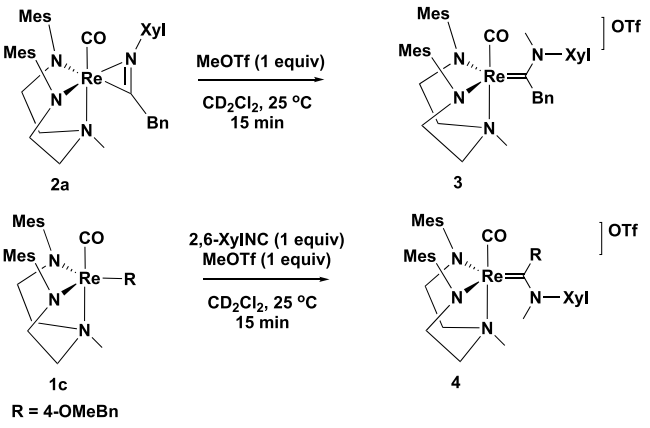


complexes are rare examples of Fisher carbene complexes generated via the treatment of an acyl or iminoacyl ligand with a Lewis or Brønsted acid. Importantly, the reaction sequence, the formation of an acyl or iminoacyl complex followed by treatment with a proton to generate a carbene as an intermediate, which subsequently rotates about the M−C (carbene) bond prior to transfer of a proton to a methyl group to form methane, may be considered in protonation reactions as described by Norton et al. for the reaction of $(Cp)_2$*$ZrMe_2$ in the presence of isocyanides, with Brønsted acids to generate [$(Cp)_2$*Zr(iminoacyl)]$^+$ + $CH_4$ (Scheme 4).[27]

**Scheme 4. Proposed Mechanism for the Reaction of $(Cp)_2$*$ZrMe_2$ in the Presence of Isocyanides with Brønsted Acids to Generate [$(Cp)_2$*Zr(iminoacyl)]$^+$ + $CH_4$**

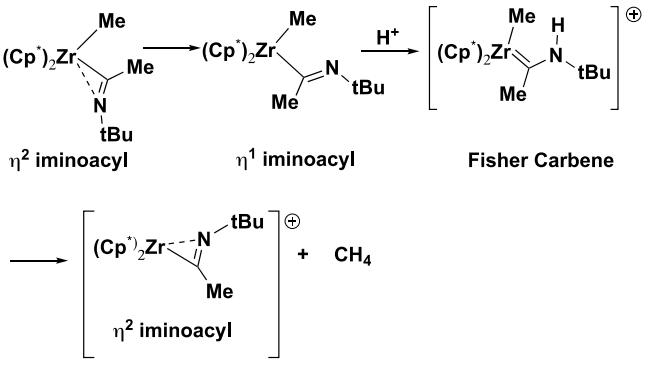


X-ray quality crystals were afforded by the slow diffusion of pentane into concentrated solutions of **3** or **4** in dichloromethane (Figures 7 and 8). The addition of the methyl group to the nitrogen atom in the iminoacyl ligands was confirmed in both structures. The rhenium center is in a distorted trigonal bipyramidal environment in both complexes ($\tau$ = 0.87 and 0.89 for **3** and **4**, respectively)[58] with Re═C distances of 2.067(8) (**3**) and 2.066(5) (**4**) Å. These bond lengths are similar to other carbene complexes reported by our laboratory, which


https://doi.org/10.1021/acs.organomet.4c00338
Organometallics 2024, 43, 3002−3012

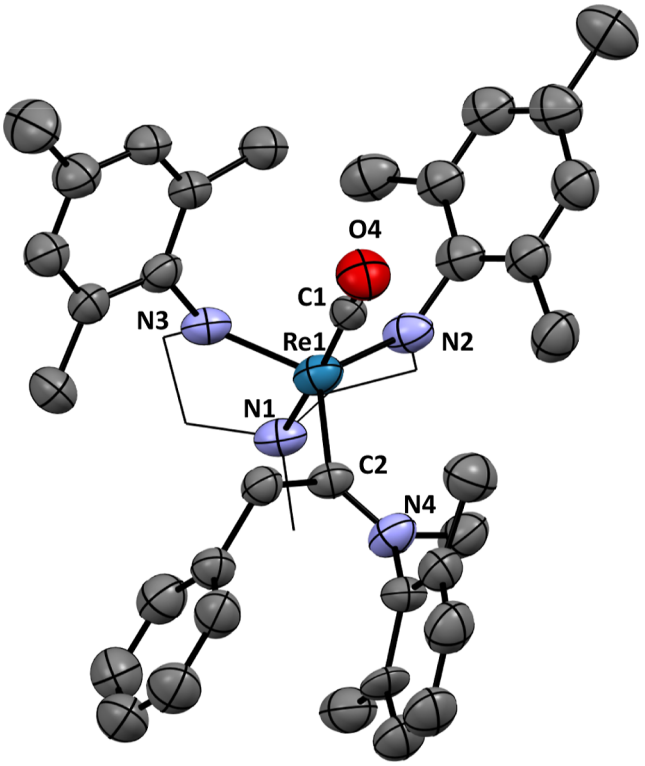


**Figure 7.** X-ray crystal structure of the cationic portion of **3**. Ellipsoids are at a 50% probability level. Hydrogen atoms were omitted, and the ligand is displayed in wireframe for clarity. The highly disordered triflate anion is also omitted for clarity. Selected bond lengths (Å) and angles (deg): Re1−C1, 1.917(9); Re1−N1, 2.219(7); Re1−N2, 1.936(7); Re1−N3, 1.922(7); Re1−C2, 2.066(7); O4−C1, 1.128(10); N4−C2, 1.303(10); N2−Re1−N1, 83.1(3); N3−Re1−N2, 118.4(3); N3−Re1−N1, 81.7(3); N3−Re1−C2, 123.4(3); N2−Re1−C2, 117.7(3); C1−Re1−N1, 99.7(3); O4−C1−Re1, 177.3(7).

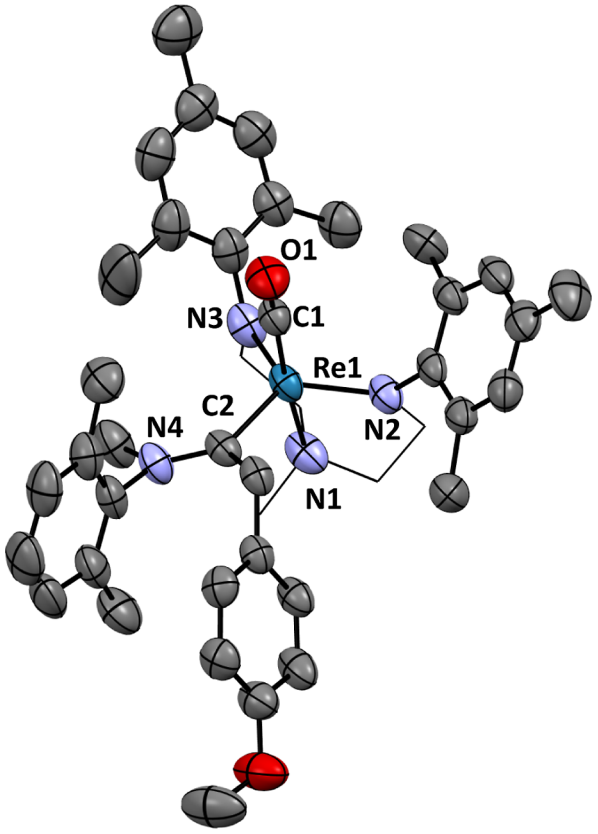


**Figure 8.** X-ray crystal structure of the cationic portion of **4**. Ellipsoids are at a 50% probability level. Hydrogen atoms were omitted, and the ligand is displayed in wireframe for clarity. The highly disordered triflate anion is also omitted for clarity. Selected bond lengths (Å) and angles (deg): Re1−C1, 1.857(4); Re1−N1, 2.281(3); Re1−N2, 1.992(3); Re1−N3, 1.925(3); Re1−C2, 2.057(4); O1−C1, 1.173(5); N4−C2, 1.256(5); N2−Re1−N1, 80.58(13); N3−Re1−N2, 112.43(13); N3−Re1−N1, 80.96(13); N3−Re1−C2, 113.02(15); N2−Re1−C2, 131.47(15); C1−Re1−N1, 175.25(14); O1−C1−Re1, 179.4(4).

were 1.980(3) Å for [(DAP)Re(O) (CC($CH_3$)$OCH_3$)][OTf] (DAP = 2,6-Bis((arylamino)methyl)pyridine; aryl = mesityl) and 2.021(2) Å for [(DAP)Re(O) (CHN$CH_3$(2,6-($CH_3$)$_2C_6H_3$))][OTf] (DAP = 2,6-Bis- ((arylamino)methyl)-pyridine; aryl = xylyl).[28]

**DFT Studies.** As noted earlier, complexes **2a** and **2d** feature different hapticities of the iminoacyl ligand. Since the only difference in these molecules is the nature of the substituent in the para position of the phenyl group (H versus OMe), this preference appears to be electronic in nature. To investigate this more thoroughly, DFT calculations (APFD) were employed.

Scheme 5 shows the general form of the optimized complexes for both $\eta^1$ and an $\eta^2$ binding mode of the iminoacyl ligand. Substituents were varied in the para position of both aryl groups in the imino acyl ligands. In Table 1, Gibbs free energies ($\Delta G^\circ$) in toluene and dichloromethane for the conversion from the $\eta^1$ form to the $\eta^2$ form are all less than 2 kcal/mol. This suggests that both isomeric forms ($\eta^1$ or $\eta^2$) are present in solution at room temperature, regardless of the polarity of the solvent. This conclusion is true regardless of the nature of the substituent, i.e., whether the substituent is electron withdrawing or electron donating, which suggests that the change in hapticity is not electronic in nature.

To investigate whether a similar result could be achieved with *tert*-butyl isocyanide, the structures in Scheme 6 were optimized. The results indicate that regardless of the initial

**Scheme 5. General form of the Iminoacyl Rhenium Complexes Optimized as $\eta^1$ and $\eta^2$**

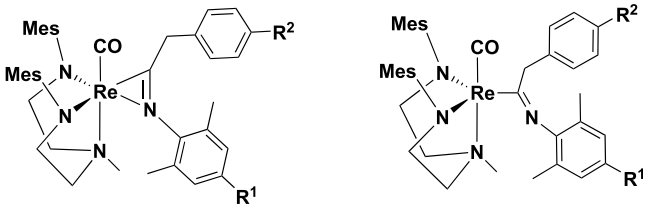


$R^1$, $R^2$: H, OMe, $NMe_2$, $NO_2$, $CF_3$

conformation of the complex ($\eta^1$ or $\eta^2$), the optimized version was always $\eta^2$.

The reaction pathways were also calculated for the reactions of 2,6-dimethylphenyl isocyanide and *tert*-butyl isocyanide with complexes **1a**, **1b**, and **1c** (Figure 9). Insertions of isocyanides into M−X bonds usually proceed by the coordination of the isocyanide ligand to the metal via the carbon lone pair. This is followed by insertion into the adjacent metal−carbon bond to form the iminoacyl complex.[1] In Figure 9, **TS1** (15.8 kcal/mol (dichloromethane)) corresponds to the activation barrier for the formation of the isocyanide complex, **6**. Complex **6** features a Re−C (isocyanide) bond of 2.08 Å and a Re−C


https://doi.org/10.1021/acs.organomet.4c00338
Organometallics 2024, 43, 3002−3012

**Table 1. APFD Calculated Energy Differences between $\eta^1$ and $\eta^2$ Complexes of Scheme 3 Using the PCM Solvation Model for Toluene (Red) and Dichloromethane (Blue)**

| entry | $R^1$ | $R^2$ | AG ($\eta^1$–$\eta^2$ (kcal/mol) |
|---|---|---|---|
| 1 | H | H | 0.8, 0.6 |
| 2 | H | OMe | 0.7, 0.6 |
| 3 | H | $NMe_2$ | 0.9, 0.7 |
| 4 | H | $CF_3$ | −0.2, −0.3 |
| 5 | H | $NO_2$ | −1.0, −1.1 |
| 6 | OMe | OMe | 1.2, 1.1 |
| 7 | $NMe_2$ | OMe | 1.4, 1.4 |
| 8 | $NO_2$ | OMe | −1.6, −1.7 |
| 9 | $CF_3$ | OMe | 0.0, 0.0 |

**Scheme 6. General Form of the Iminoacyl Rhenium Complexes Optimized as $\eta^1$ and $\eta^2$**

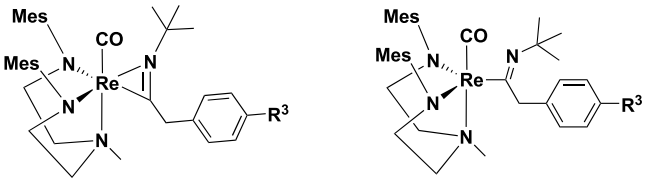


$R^3$: H, OMe, $NMe_2$, $NO_2$, $CF_3$

(benzyl) bond of 2.23 Å. Prior to insertion, the Re−C (benzyl) bond lengthens (2.38 Å) through **TS2** (2.0 kcal/mol) to afford the $\eta^1$-iminoacyl, **8**, which features a long Re−N (xylyl) bond (3.19 Å). This complex rearranges to the $\eta^2$-iminoacyl **2a**, which was observed experimentally. Importantly, the calculated stereochemistry of **2a** is consistent with its crystal structure with the substituent on the iminoacyl nitrogen (xylyl) on the same side as the in-plane mesityl group.

Similar pathways were calculated for insertion into Re−C (methyl), **1b** and Re−C (4-methoxybenzyl), **1c** and **1d** (Supporting Information). These results are consistent with experimental observations and suggest that the complex with the bulkier isocyanide, 2,6-dimethylphenyl isocyanide, is thermodynamically stable in either coordination mode whereas the less bulky *tert*-butyl group prefers $\eta^2$ coordination.

## CONCLUSIONS

The insertion of isocyanides into Re−R ($R$ = methyl, benzyl) bonds results in $\eta^1$ or $\eta^2$ iminoacyls. In the case of 2,6-dimethylphenylisocyanide, the experimental and DFT data suggest that the resulting iminoacyl complexes can adopt $\eta^1$ or $\eta^2$ binding modes. When *tert*-butyl isocyanide was employed, $\eta^2$ coordination of the iminoacyl complex was exclusively observed. Experimental and computational results suggest that the preference for hapticity is likely the result of steric effects and not a consequence of electronic preferences.

Treatment of the resultant iminoacyls with Lewis and Brønsted acids results in the isolation of Fisher carbenes. These species may be considered as viable intermediates in reactions such as alkyl abstractions and alkane formation that are common for transition-metal alkyls and isocyanides in the presence of Brønsted and Lewis acids.

## EXPERIMENTAL SECTION

**General Considerations.** Complex **1b** was prepared as previously reported.[28] Reagents 2,6-dimethylphenyl isocyanide, *tert*-butyl isocyanide, and Grignard reagents RMgCl (R=Bn (1 M in diethyl ether) and $R$ = 4-OMeBn (0.25 M in tetrahydrofuran)) were purchased from Sigma-Aldrich and used as received. Anhydrous

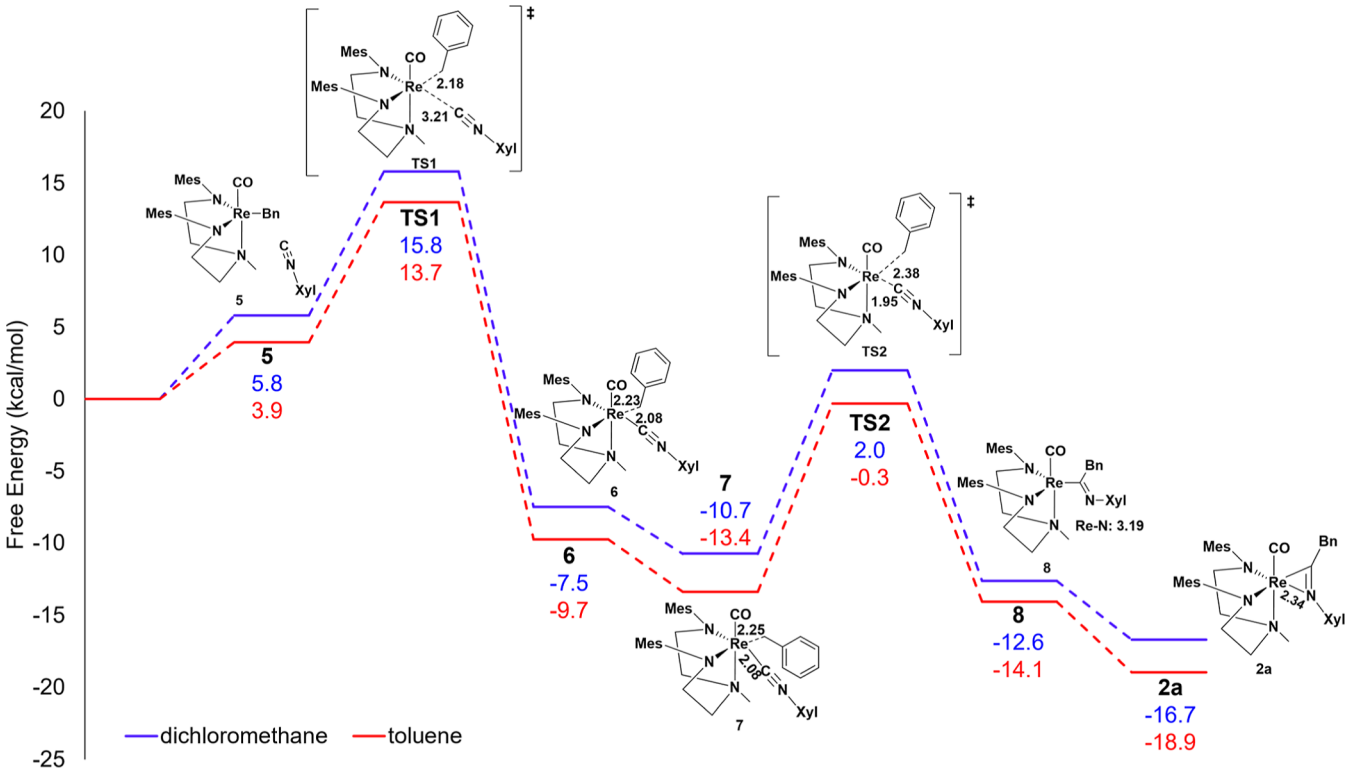


**Figure 9.** APFD calculated pathway for the insertion of 2,6-dimethylphenyl isocyanide into the rhenium-benzyl bond of **1a**. The solvated energies are reported using the PCM solvation model for dichloromethane (blue) and toluene (red).



https://doi.org/10.1021/acs.organomet.4c00338
Organometallics 2024, 43, 3002−3012

solvents and deuterated solvents were purchased from Sigma-Aldrich and Cambridge Isotope Laboratories, respectively, and dried with molecular sieves before use. $^{1}$H, $^{13}$C, HMBC, DEPT, and DEPT135 spectra were obtained in the Molecular Education, Technology and Research Innovation Center (METRIC) at NC State University on 500, 600, or 700 MHz spectrometers at room temperature. Chemical shifts are listed in parts per million (ppm) and are referenced to the deuterated solvents peaks. Elemental analyses were performed by Atlantic Micro Laboratories, Inc. FTIR spectra were obtained for KBr thin films. X-ray crystallography was performed on a Bruker Venture D8 instrument in the METRIC facility at NCSU.

**Synthesis of (CO)Re(DAAm) (R) (DAAm = *N*$^1$-Mesityl-*N*$^2$-(2-(mesitylamino)-ethyl)-*N*$^2$-methylethane-1,2-diamine) (1) (R═Bn (1a), 4-OMeBn (1c)).** (CO)Re(DAAm) (OAc)[37] (200 mg, 0.32 mmol) was added to a 20 mL scintillation vial charged with a small stir bar, followed by the addition of 5−10 mL of dry dichloromethane. Ten equiv of appropriate Grignard reagent (RMgCl, R═Bn (3.2 mL, 3.2 mmol); 4-OMeBn (13 mL, 3.2 mmol)) was added to the vial dropwise and stirred at room temperature overnight under a nitrogen atmosphere. Upon completion of the reaction, water was added dropwise, and a liquid−liquid extraction was performed with dichloromethane three times. The combined organic layers were washed with brine, dried over $Na_2SO_4$, and the solvent was removed under vacuum to give crude product. The crude product was dissolved in a minimum amount of dichloromethane, and excess pentane was added to precipitate the product, which was filtered and dried to afford orange solids.

**General Synthesis of the Iminoacyl Complexes.** The rhenium alkyl or benzyl complex described above (**1a**, **1b**, or **1c**) was placed in a screw cap NMR tube, and 0.7 mL of deuterated dichloromethane was added to dissolve the complex. Equimolar amounts of the isocyanide reagent (2,6-dimethylphenyl isocyanide or *tert*-butyl isocyanide) were added to the solution, and the mixture was shaken well. $^{1}$H NMR spectroscopy confirmed the product formation after 15 min. The product was crystallized by using dichloromethane and pentane to give red or orange crystals.

**Synthesis of [(CO) (DAAm-Mes)Re(Bn)], (DAAm = *N*$^1$-Mesityl-*N*$^2$-(2-(mesitylamino)-ethyl)-*N*$^2$-methylethane-1,2-diamine) (1a).** Following the general synthesis, complex **1a** was obtained in quantitative yield as an orange powder. $^{1}$H NMR (300 MHz, $CD_2Cl_2$): $\delta$:7.10 (t, $J$ = 7.7 Hz, 2H), 6.97 (d, $J$ = 7.2 Hz, 2H), 6.87 (t, $J$ = 7.3 Hz, 1H), 6.82 (s, 4H), 3.63 (tt, $J$ = 13.8, 6.9 Hz, 4H), 3.16 (dt, $J$ = 11.4, 5.5 Hz, 2H), 3.05 (s, 3H), 3.04−3.00 (m, 2H), 2.99 (s, 2H), 2.27 (s, 2H), 2.15 (s, 2H), 2.06 (s, 2H) $^{13}$C{$^{1}$H} NMR (151 MHz, $CD_2Cl_2$): $\delta$ 201.38, 157.79, 153.23, 134.48, 132.43, 130.91, 129.19, 129.08, 128.66, 127.55, 123.74, 62.14, 59.59, 46.14, 45.25, 20.90, 19.76, 19.41. IR (FTIR, cm$^{-1}$): $\nu$(CO) 1856. Anal calc. for $C_{31}H_{40}N_3ORe$: C, 56.68; N, 6.40; H, 6.14; found: C, 56.83; N, 6.41; H, 6.11.

*Synthesis of [(CO) (DAAm-Mes)Re(4-OMeBn)], (DAAm = N$^1$-Mesityl-N$^2$-(2-(mesitylamino)-ethyl)-N$^2$-methylethane-1,2-diamine) (**1c**).* Following the general synthesis, complex **1c** was obtained in quantitative yield as an orange powder. $^{1}$H NMR (600 MHz, $CD_2Cl_2$): $\delta$: 6.81 (d, $J$ = 8.6 Hz, 2H, 4-OMe-Bn ortho-H), 6.74 (s, 4H, Mes Ar H), 6.59 (d, $J$ = 8.7 Hz, 2H, 4-OMe-Bn ortho-H), 3.63 (s, 3H, −$OCH_3$), 3.60−3.49 (m, 4H, MesDAAm−$CH_2$− × 2), 3.07 (dt, $J$ = 11.4, 5.6 Hz, 2H, MesDAAm−$CH_2$−), 2.97−2.91 (m, 5H, overlapping N−$CH_3$ and MesDAAm−$CH_2$−), 2.89 (s, 2H, Re-$CH_2$−Ph), 2.19 (s, 6H, Mes $CH_3$), 2.07 (s, 6H, Mes $CH_3$), 1.97 (s, 6H, Mes $CH_3$). $^{13}$C{$^{1}$H} NMR (151 MHz, $CD_2Cl_2$): $\delta$ 201.57, 157.83, 156.80, 145.04, 134.44, 132.47, 130.95, 129.49, 129.19, 129.06, 112.97, 62.06, 59.59, 55.59, 46.10, 44.57, 20.90, 19.72, 19.40. Anal calcd for $C_{32}H_{42}N_3O_2Re$: C, 55.95; H, 6.16; N, 6.12; found: C, 55.90; H, 5.99; N, 6.26.

*Synthesis of (CO)Re(DAAm) (C(Bn)N(2,6-Xyl)) (DAAm = N$^1$-Mesityl-N$^2$-(2-(mesitylamino)-ethyl)-N$^2$-methylethane-1,2-diamine) (**2a**).* This complex was prepared using the procedure for general synthesis of the iminoacyl complex described above. Complex **1a** (15.0 mg, 0.0230 mmol) and 2,6-dimethylphenyl isocyanide (3.00 mg, 0.0230 mmol) were combined to afford a red crystalline product (13.0 mg, 62.0% yield). $^{1}$H NMR (700 MHz, $CD_2Cl_2$): $\delta$ 7.07 (d, $J$ = 7.3 Hz, 3H), 6.86−6.82 (m, 4H), 6.82−6.79 (m, 5H), 3.88 (s, 2H), 3.81 (dt, $J$ = 13.6, 5.7 Hz, 2H), 3.68 (dt, $J$ = 13.8, 5.6 Hz, 2H), 3.16 (dt, $J$ = 11.4, 5.4 Hz, 2H), 3.01 (dt, $J$ = 11.3, 5.5 Hz, 2H), 2.89 (s, 3H), 2.29 (s, 6H), 2.26 (s, 6H), 2.16 (s, 6H), 1.79 (s, 6H). $^{13}$C{$^{1}$H} NMR (151 MHz, $CD_2Cl_2$): $\delta$ 233.99, 202.20, 157.38, 137.28, 134.31, 133.05, 131.87, 130.09, 129.40, 129.21, 128.57, 128.36, 126.19, 62.14, 59.67, 49.12, 48.48, 20.86, 20.43, 20.11, 19.55. IR (FTIR, cm$^{-1}$): $_V$(CO) 1834 $_V$(CNR) 1600. Elemental analysis: ($C_{40}H_{49}N_4ORe$)·1/3($CH_2Cl_2$) theory: (C: 59.34, H: 6.13, N: 6.86);found: (C: 59.38, H: 6.13, N: 6.89).

*Synthesis of (CO)Re(DAAm) (C($CH_3$)NC($CH_3$)$_3$) (DAAm = N$^1$-Mesityl-N$^2$-(2-(mesitylamino)-ethyl)-N$^2$-methylethane-1,2-diamine) (**2b**).* This complex was prepared using the same procedure as **2a**. 1.9 mL (0.017 mmol) of *tert*-butyl isocyanide was added to the solution of **1c** (10 mg, 0.017 mmol) in $CD_2Cl_2$ to afford an orange crystal as the product (5.0 mg, 38% yield). $^{1}$H NMR (500 MHz, $CD_2Cl_2$): $\delta$ 6.83 (s, 2H), 6.74 (s, 2H), 3.67 (dt, $J$ = 12.2, 5.6 Hz, 2H), 3.57−3.50 (m, 2H), 3.06 (dt, $J$ = 11.3, 5.5 Hz, 2H), 2.79 (dt, $J$ = 11.5, 5.5 Hz, 2H), 2.64 (s, 3H), 2.49 (s, 3H), 2.33 (s, 6H), 2.25 (s, 6H), 2.04 (s, 6H), 1.39 (s, 9H). $^{13}$C{$^{1}$H} NMR (176 MHz, $CD_2Cl_2$): $\delta$ 224.63, 202.92, 158.01, 158.00, 132.99, 132.00, 131.86, 129.13, 128.94, 62.59, 60.83, 54.84, 48.24, 30.73, 27.59, 20.84, 20.06, 19.97. IR (FTIR, cm$^{-1}$): $_V$(CO) 1826 $_V$(CNR) 1616. Elemental analysis: ($C_{30}H_{45}N_4ORe$)·1/4($CH_2Cl_2$). Theory: (C: 53.03, H: 6.69, N: 8.18); found: (C: 53.56, H: 6.81, N: 8.16).

*Synthesis of (CO)Re(DAAm) (C(4-OMeBn)NC($CH_3$)$_3$) (DAAm = N$^1$-Mesityl-N$^2$-(2-(mesitylamino)-ethyl)-N$^2$-methylethane-1,2-diamine) (**2c**).* This complex was prepared using the same procedure as that for **2a**, with 15 mg of **1b** (0.022 mmol) and 2.5 mL of *tert*-butyl isocyanide (0.022 mmol) reacting together to afford an orange crystal product (9.0 mg, 54% yield). $^{1}$H NMR (600 MHz, $CD_2Cl_2$): $\delta$ 7.13 (d, $J$ = 8.3 Hz, 2H), 6.78 (s, 2H), 6.75 (d, $J$ = 3.7 Hz, 2H), 6.73 (s, 2H), 4.43 (s, 2H), 3.74 (s, 3H), 3.72−3.68 (m, 2H), 3.55−3.50 (m, 2H), 3.11−3.05 (m, 2H), 2.76−2.68 (m, 2H), 2.53 (s, 3H), 2.27 (s, 6H), 2.23 (s, 6H), 2.04 (s, 6H), 1.41 (s, 9H). $^{13}$C{$^{1}$H} NMR (176 MHz, $CD_2Cl_2$): $\delta$ 223.50, 204.30, 158.63, 158.03, 132.72, 131.85, 130.94, 129.21, 128.99, 128.91, 114.41, 114.20, 63.27, 61.41, 55.64, 55.31, 49.49, 43.07, 31.69, 31.19, 20.81, 20.15.

*Synthesis of (CO)Re(DAAm) (C(4-OMeBn)N(2,6-Xyl)) (DAAm = N$^1$-Mesityl-N$^2$-(2-(mesitylamino)-ethyl)-N$^2$-methylethane-1,2-diamine) (**2d**).* This complex was prepared using the same procedure as for **2a**, with (15 mg, 0.022 mmol) of **1b** and (3.0 mg, 0.022 mmol) of 2,6-dimethylphenyl isocyanide to afford an orange crystal product (10 mg, 46% yield). $^{1}$H NMR (700 MHz, $CD_2Cl_2$): $\delta$ 6.86 (d, $J$ = 7.4 Hz, 2H), 6.85−6.78 (m, 5H), 6.69 (d, $J$ = 9.0 Hz, 2H), 6.61 (d, $J$ = 8.1 Hz, 2H), 3.82−3.78 (m, 4H), 3.71 (s, 3H), 3.69−3.65 (m, 2H), 3.19−3.11 (m, 2H), 3.01 (dt, $J$ = 12.0, 4.9 Hz, 2H), 2.87 (s, 3H), 2.28 (s, 6H), 2.26 (s, 6H), 2.15 (s, 6H), 1.80 (s, 6H). $^{13}$C{$^{1}$H} NMR (176 MHz, $CD_2Cl_2$): $\delta$ 234.36, 202.33, 158.36, 157.41, 148.89, 134.31, 133.09, 131.90, 131.06, 129.42, 129.22, 128.61, 122.61, 113.81, 62.13, 59.69, 55.69, 48.50, 34.69, 22.91, 20.85, 20.42, 20.17, 19.58, 14.38. IR (FTIR, cm$^{-1}$): $_V$(CO) 1841 $_V$(CNR) 1684. Elemental analysis: ($C_{41}H_{51}N_4O_2Re$)·1/2($CH_2Cl_2$). Theory: (C: 57.92, H: 6.09, N: 6.51); found: (C: 58.17, H: 6.09, N: 6.32).

*Synthesis of [(CO)Re(DAAm) (C(Bn)N($CH_3$) (2,6-Xyl))][OTf] (DAAm = N$^1$-Mesityl-N$^2$-(2-(mesitylamino)-ethyl)-N$^2$-methylethane-1,2-diamine) (**3**).* In a 25 mL scintillation vial, **2a′** (272 mg, 0.35 mmol) was dissolved in dichloromethane, followed by the dropwise addition of an equimolar amount of methyl triflate (38 mL, 0.35 mmol). The mixture was allowed to stir at room temperature for 10 min, and upon the completion of the reaction, excess pentane was added to precipitate the product. After filtration and drying under vacuum, an orange powder was afforded as the desired product (193 mg, 59% yield). $^{1}$H NMR (600 MHz, $CD_2Cl_2$): $\delta$ 7.14 (t, $J$ = 7.6 Hz, 1H), 7.07 (t, $J$ = 7.5 Hz, 1H), 7.04−6.98 (m, 2H), 6.96−6.91 (m, 3H), 6.84 (d, $J$ = 6.2 Hz, 2H), 6.72−6.71 (m, 1H), 6.27 (d, $J$ = 7.1 Hz, 2H), 4.33 (ddd, $J$ = 14.3, 7.0, 3.3 Hz, 1H), 4.11 (dtd, $J$ = 14.6, 5.4, 3.5 Hz, 2H), 3.87 (ddd, $J$ = 14.3, 8.8, 4.7 Hz, 1H), 3.73 (s, 3H), 3.66 (d, $J$ = 16.0 Hz, 1H), 3.61 (dt, $J$ = 12.8, 4.3 Hz, 2H), 3.53 (s, 3H), 3.46−3.40 (m, 2H), 3.31 (d, $J$ = 16.1 Hz, 1H), 2.61 (s, 3H), 2.34 (s, 3H), 2.23 (s, 3H), 2.15 (s, 3H), 1.99 (s, 6H), 1.90 (s, 3H), 1.80 (s,


https://doi.org/10.1021/acs.organomet.4c00338
Organometallics 2024, 43, 3002−3012

3H). $^{13}C\{^1H\}$ NMR (151 MHz, $CD_2Cl_2$): δ 263.03, 198.91, 156.89, 156.41, 143.54, 136.87, 136.29, 134.14, 133.08, 132.89, 132.30, 131.27, 130.75, 130.67, 130.54, 130.37, 130.28, 129.96, 129.91, 128.68, 127.71, 65.61, 64.66, 61.87, 59.17, 53.30, 45.10, 34.69, 23.35, 22.90, 21.44, 20.83, 20.70, 19.41, 18.81, 18.47, 18.19, 14.38. IR (FTIR, $cm^{-1}$): $_V$(CO) 1908. Elemental analysis: ($C_{41}H_{52}N_4ORe{\cdot}CF_3O_3S^-$) Theory: (C: 52.93, H: 5.46, N: 5.88); found: (C: 52.64, H: 5.45, N: 5.71).

*Synthesis of [(CO)Re(DAAm) (C(4-OMeBn)N(CH$_3$) (2,6-Xyl))][OTf] (DAAm = N$^1$-Mesityl-N$^2$-(2-(mesitylamino)-ethyl)-N$^2$-methyl-ethane-1,2-diamine) (**4**).* This complex was prepared by reacting **1b** (15 mg, 0.022 mmol) with 2,6-dimethylphenyl isocyanide (3.0 mg, 0.022 mmol) and 2.4 mL (0.022 mmol) of methyl triflate to afford a deep orange crystal (15 mg, 68% yield). $^1H$ NMR (600 MHz, $CD_2Cl_2$): δ 7.18 (t, *J* = 7.6 Hz, 1H), 7.05 (d, *J* = 7.6 Hz, 1H), 7.01 (s, 1H), 6.93 (s, 2H), 6.85 (s, 1H), 6.73 (d, *J* = 2.1 Hz, 1H), 6.46 (d, *J* = 8.6 Hz, 2H), 6.13 (d, *J* = 8.6 Hz, 2H), 4.35−4.27 (m, 1H), 4.15−4.07 (m, 2H), 3.87 (ddd, *J* = 14.5, 8.9, 4.8 Hz, 1H), 3.73 (s, 3H), 3.69 (s, 3H), 3.64−3.59 (m, 2H), 3.55 (s, 1H), 3.52 (s, 3H), 3.46−3.41 (m, 2H), 3.28 (d, *J* = 16.0 Hz, 1H), 2.61 (s, 3H), 2.35 (s, 3H), 2.24 (s, 3H), 2.16 (s, 3H), 2.02 (s, 3H), 1.97 (s, 3H), 1.90 (s, 3H), 1.86 (s, 3H). $^{13}C\{^1H\}$ NMR (151 MHz, $CD_2Cl_2$): δ 263.47, 198.94, 159.33, 156.87, 156.36, 143.57, 136.88, 136.29, 134.11, 133.07, 132.33, 131.20, 130.76, 130.68, 130.53, 130.43, 130.38, 130.30, 129.98, 128.72, 124.70, 113.96, 65.62, 64.62, 61.86, 59.15, 55.76, 53.29, 44.11, 23.36, 21.45, 20.82, 20.71, 19.41, 18.86, 18.50, 18.16. IR (FTIR, $cm^{-1}$): $_V$(CO) 1897. Elemental analysis: ($C_{42}H_{54}N_4O_2Re{\cdot}CF_3O_3S^-$)·1/2($CH_2Cl_2$) Theory: (C: 50.99, H: 5.41, N: 5.47); found: (C: 50.99, H: 5.46, N: 5.35).

**Computational Studies.** The calculations performed for this work were performed using the Gaussian 16[59] computational program. Geometry and transition state optimizations were performed with two different basis sets: 6-31G(d,p)[60,61] and SDD[62−64] with an added f polarization function[65] on light atoms and rhenium, respectively. In the optimization calculations, tight optimization criteria (opt = tight) in the Gaussian 16[59] implementation of APFD[66] with an ultrafine integral grid (int = ultrafine) was employed. To find a zeroth-order (local minimum) or first-order (transition state) saddle point, analytical frequency calculations were performed on all structures after they were fully optimized. Each transition state had two minima associated with it, and they were found by an animation of the imaginary frequency. For the energy calculations, the same basis set for geometry and transition state optimizations on rhenium was used, but for the light atoms, the basis set was 6-311++G(d,p).[67] All energy values were calculated at 298 K and used the polarizable continuum model (PCM) method[68,69] to include solvation corrections. The chosen solvents were dichloromethane and toluene.

## ■ ASSOCIATED CONTENT

### Supporting Information

The Supporting Information is available free of charge at https://pubs.acs.org/doi/10.1021/acs.organomet.4c00338.

Additional X-ray experimental details; $^1H$,$^{13}C$ NMR; further computational details, pathways, and optimized structures (PDF)

Optimized geometries (XYZ)

### Accession Codes

Deposition Numbers 2329226−2329235 contain the supplementary crystallographic data for this paper. These data can be obtained free of charge via the joint Cambridge Crystallographic Data Centre (CCDC) and Fachinformationszentrum Karlsruhe Access Structures service.

## ■ AUTHOR INFORMATION


### Corresponding Author

**Elon A. Ison** − *Department of Chemistry, North Carolina State University, Raleigh, North Carolina 27695-8204, United States;* orcid.org/0000-0002-2902-2671; Email: eaison@ncsu

### Authors

**Liana Pauly** − *Department of Chemistry, North Carolina State University, Raleigh, North Carolina 27695-8204, United States*

**Abdullahi K. Adegboyega** − *Department of Chemistry, North Carolina State University, Raleigh, North Carolina 27695-8204, United States*

**Caleb A. Brown** − *Department of Chemistry, North Carolina State University, Raleigh, North Carolina 27695-8204, United States*

**Damaris E. Pérez** − *Department of Chemistry, North Carolina State University, Raleigh, North Carolina 27695-8204, United States*

Complete contact information is available at: https://pubs.acs.org/10.1021/acs.organomet.4c00338


### Notes

The authors declare no competing financial interest.

## ■ ACKNOWLEDGMENTS

We acknowledge the NCSU Office of Information Technology (OIT) High Performance Computing (HPC) for computational support. This work was supported by the National Science Foundation (CHE-2154878). Funding for D8 VENTURE acquisition was provided in part by North Carolina Biotechnology Center grant: NCBC#2019-IDG-1010.

## ■ REFERENCES


(1) Boyarskiy, V. P.; Bokach, N. A.; Luzyanin, K. V.; Kukushkin, V. Y. Metal-Mediated and Metal-Catalyzed Reactions of Isocyanides. *Chem. Rev.* **2015**, *115*, 2698−2779.

(2) Lygin, A. V.; De Meijere, A. Isocyanides in the Synthesis of Nitrogen Heterocycles. *Angew. Chemie - Int. Ed.* **2010**, *49*, 9094−9124.

(3) Ruijter, E.; Vlaar, T.; Ruijter, E.; Maes, B. U. W.; Orru, R. V. A. Palladium-Catalyzed Migratory Insertion of Isocyanides: An Emerging Platform in Cross-Coupling. *Chemistry* **2013**, *2*, 7084−7097.

(4) Collet, J. W.; Roose, T. R.; Ruijter, E.; Maes, B. U. W.; Orru, R. V. A. Base Metal Catalyzed Isocyanide Insertions. *Angew. Chem.* **2020**, *132*, 548−566.

(5) Knorr, M.; Jourdain, I.; Braunstein, P.; Strohmann, C.; Tiripicchio, A.; Ugozzoli, F. Insertion Reactions of Alkynes and Organic Isocyanides into the Palladium-Carbon Bond of Dimetallic Fe-Pd Alkoxysilyl Complexes. *Dalt. Trans.* **2006**, No. 44, 5248−5258.

(6) Han, Y.; Huynh, H. V. Mixed Carbene − Isocyanide Pd (II) Complexes: Synthesis, Structures and Reactivity towards Nucleophiles †. **2009**, 2201−2209. DOI: .

(7) Qiu, G.; Ding, Q.; Wu, J. Recent Advances in Isocyanide Insertion Chemistry. *Chem. Soc. Rev.* **2013**, *42*, 5257−5269.

(8) Lang, S. Unravelling the Labyrinth of Palladium-Catalysed Reactions Involving Isocyanides. *Chem. Soc. Rev.* **2013**, *42*, 4867−4880.

(9) Amor, F.; Sánchez-Nieves, J.; Royo, P.; Jacobsen, H.; Blacque, O.; Berke, H.; Lanfranchi, M.; Pellinghelli, M. A.; Tiripicchio, A. Competitive Insertion of Isocyanide into Tantalum-Amido and Tantalum-Methyl Bonds. *Eur. J. Inorg. Chem.* **2002**, *2002*, 2810−2817.

(10) Sebastián, A.; Royo, P.; Gómez-Sal, P.; Ramírez de Arellano, C. Diastereoselective Insertion of Isocyanide into the Alkyl-Metal Bond of Methylbenz[e]Indenyl Ansa-Zirconocene Complexes. *Eur. J. Inorg. Chem.* **2004**, *2004*, 3814−3821.

(11) Massarotti, A.; Brunelli, F.; Aprile, S.; Giustiniano, M.; Tron, G. C. Medicinal Chemistry of Isocyanides. *Chem. Rev.* **2021**, *121*, 10742−10788.

(12) Martins, A. M.; Ascenso, J. R.; De Azevedo, C. G.; Dias, A. R.; Duarte, M. T.; Da Silva, J. F.; Veiros, L. F.; Rodrigues, S. S. Insertion of Isocyanides into Group 4 Metal-Carbon and Metal-Nitrogen Bonds. Syntheses and DFT Calculations. *Organometallics* **2003**, *22*, 4218−4228.
(13) Thomson, R. K.; Schafer, L. L. Synthesis, Structure, and Insertion Reactivity of Zirconium and Hafnium Amidate Benzyl Complexes. *Organometallics* **2010**, *29*, 3546−3555.
(14) Barnea, E.; Andrea, T.; Berthet, J. C.; Ephritikhine, M.; Eisen, M. S. Coupling of Terminal Alkynes and Isonitriles by Organoactinide Complexes: Scope and Mechanistic Insights. *Organometallics* **2008**, *27*, 3103−3112.
(15) Becker, T. M.; Alexander, J. J.; Bauer, J. A. K.; Nauss, J. L.; Wireko, F. C. CNR and CO Insertion Reactions of 2,6-Xylyl Isocyanide with p -Chlorobenzylpentacarbonylmanganese. *Organometallics* **1999**, *18*, 5594−5605.
(16) (a) Kinzhalov, M. A.; Boyarskii, V. P. Structure of Isocyanide Palladium(II) Complexes and Their Reactivity toward Nitrogen Nucleophiles. *Russ. J. Gen. Chem.* **2015**, *85*, 2313−2333. (b) Zhuo, Q.; Yang, J.; Zhou, X.; Shima, T.; Luo, Y.; Hou, Z. Dinitrogen Cleavage and Multicoupling with Isocyanides in a Dititanium Dihydride Framework. *J. Am. Chem. Soc.* **2024**, *146*, 10984−10992.
(17) Vlaar, T.; Ruijter, E.; Maes, B. U. W.; Orru, R. V. A. Palladium-Catalyzed Migratory Insertion of Isocyanides: An Emerging Platform in Cross-Coupling Chemistry. *Angew. Chemie - Int. Ed.* **2013**, *52*, 7084−7097.
(18) Crabtree, R. H. *The Organometallic Chemistry of the Transition Metals*; wiley, 1948; Vol. *37*..
(19) Durfee, L. D.; Rothwell, I. A. N. P. Chemistry of $\eta^2$-Acyl, $\eta^2$-Iminoacyl, and Related Functional Groups. *Chem. Rev.* **1988**, *88*, 1059−1079.
(20) (a) Alexander, J. J.; Padolik, L. L.; Ho, D. M. Insertion of Isocyanides into Re-C Bonds. *Inorg. Chim. Acta* **1995**, *240*, 495−501. (b) Chen, J.; Yassin, N.; Gunasekara, T.; Norton, J. R.; Rauch, M. Insertion of Isonitriles into the M−C Bonds of Group 4 Dialkyl Complexes. *J. Am. Chem. Soc.* **2018**, *140*, 8980−8989.
(21) Fachinetti, G.; Floriani, C.; Marchetti, F.; Merlino, S. Reversible Carbonylation of Dialkylbiscyclopentadienylzirconium(IV): Synthesis and Structure of n-Acyl Derivatives of Zirconium and X-Ray Structure of Biscyclopentadienyl(n-Acetyl)Methylzirconium. *Chem. Commun.* **1976**, *1540*, 160−161.
(22) Gilbert, B. C.; Larkin, J. P.; Norman, R. C.; Perkin, J. C. S. O. C. The Formation of Stereoisomeric (H2-Aroyl)Arylbis(H5-Cyclopentadienyl)Zirconium(IV) Compounds. *J. Chem. Soc., Perkin Trans.* **1978**, *2*, 605−606.
(23) Longato, B.; Norton, J. R.; Collins, F.; Huffman, J. C.; Marsella, J. A.; Caulton, K. G. A Bridging Acetyl Group from the Reaction of a Dinuclear Methyl Complex with Carbon Monoxide. *J. Am. Chem. Soc.* **1981**, 103−209.
(24) Marsella, J. A.; Huffman, J. C.; Caulton, K. G.; Longato, B.; Norton, J. R. Dinuclear Elimination as a Route to Unusual Bridging Carbonyls and Acetyls in Heterobimetallic Complexes; J. Am. Chem. Soc., 1982; pp 6360−6368.
(25) Longato, B.; Martin, B. D.; Norton, J. R.; Anderson, O. P. Synthesis and Solution Properties of the Heterobimetallic Complexes $Cp_2ZrMe(/t\text{-}OC)M(CO)_2Cp$ (M = Cr, Mo, W) and of Their Carbonylation Derivatives. Structure of $Cp_2ZrMe(\hat{}\text{-}OC)Mo(CO)_2Cp$. *Inorg. Chem.* **1985**, *24*, 1389−1394.
(26) Lauher, J. W.; Hoffmann, R. Structure and Chemistry of Bis(Cyclopentadienyl)-MLn Complexes. *J. Am. Chem. Soc.* **1976**, *98*, 1729−1742.
(27) Chen, J.; Chen, T.; Norton, J. R.; Rauch, M. Insertion of Isonitriles into the Zr-$CH_3$ Bond of $Cp^*_2Zr(CH_3)_2$ and Electrophilic Cleavage of the Remaining Methyl Group. *Organometallics* **2018**, *37*, 4424−4430.
(28) Brown, C. A.; Lilly, C. P.; Lambic, N. S.; Sommer, R. D.; Ison, E. A. Synthesis and Reactivity of Re(III) and Re(V) Fischer Carbenes. *Organometallics* **2020**, *39*, 388−396.
(29) Tamm, M.; Hahn, F. E. Reactions of $\beta$-Functional Phenyl Isocyanides. *Coord. Chem. Rev.* **1999**, *182*, 175−209.
(30) Prest, D. W.; Mays, M. J.; Raithby, P. R.; Raithby, P. R.; Road, L.; W, C. C. B. E. The Reactivity of the Unsaturated Dimeric Rhenium Complexes $[Re_2H_2(CO)_6\{(EtO)_2POP(OEt)_2\}]$ and $[Re_2H_2(CO)_6(Ph_2PCH_2PPh_2)]$: X-Ray Crystal Structure of $[Re_2H\text{-}(CO)_6(Ph_2PCH_2PPh_2)\{g\text{-}NC(H)Me\}]$. *Dalt. Trans.* **1982**, 2021−2028.
(31) Mays, M. J.; Prest, D. W.; Raithby, P. R.; Martin, B.; Mays, J.; Road, L.; Cb, C. Structure and Reactivity of a Dimetallic Rhenium Hydride Complex with a Rhenium-Rhenium Double Bond: X-Ray Crystal Structures of $[Re_2(CO)_6(Ph_2PCH_2PPh_2)H_2]$ and $[Re_2(CO)_6(Ph_2PCH_2PPh_2)\text{-}(NCHMe)H]$. *J.C.S. Chem. Comm.* **1980**, *3*, 171−173.
(32) Adams, R. D.; Golembeski, N. M. Isocyanide Insertion Reactions and Their Role in the Cluster-Catalyzed Hydrogenation of Isocyanide Molecules. *J. Am. Chem. Soc.* **1979**, *101*, 2579−2587.
(33) Zolk, R.; Werner, H. Stepwise Formation of a Dinuclear P-Aminocarbyne- and a p-Formimidoyl-Metal Complex by Insertion of Methyl Isocyanide into an MHM Bridge. *Angew. Chem., Int. Ed. Engl.* **1985**, *2*, 577−579.
(34) Ruiz, M. A. Insertion, Rearrangement, and Coupling Processes in the Reactions of the Unsaturated Hydride Complex $[W_2(H_5\text{-}C_5H_5)_2(H)(\mu\text{-}PCy_2)(CO)_2]$ with Isocyanides. *Organometallics* **2013**, *2*, 4543−4555.
(35) Davis, J. M.; Whitby, R. J.; Jaxa-Chamiec, A. Formation of Zirconocene $H_2$-Imine Complexes by Rearrangement of Cyclic Iminoacyl Complexes. *Tetrahedron Lett.* **1992**, *33*, 5655−5658.
(36) Adams, R. D.; Chodosh, D. F. Isocyanide Insertion Reactions. 2. Structural and Dynamical Stereochemistry of $\eta^1$- and $\eta^2$-Iminoacyl Ligands. *Inorg. Chem.* **1978**, *17*, 41−48.
(37) Smeltz, J. L.; Boyle, P. D.; Ison, E. A. Mechanism for the Activation of Carbon Monoxide via Oxorhenium Complexes. *J. Am. Chem. Soc.* **2011**, *133*, 13288−13291.
(38) Thorn, M. G.; Lee, J.; Fanwick, P. E.; Rothwell, I. P. Synthesis, Structure and Molecular Dynamics of $H_2$-Iminoacyl Compounds $[Cp(ArO)Zr(H_2\text{-}ButNCCH_2Ph)(CH_2Ph)]$ and $[Cp(ArO)Zr(H_2\text{-}ButNCCH_2Ph)_2]$. *Dalt. Trans.* **2002**, 3398−3405.
(39) To, G. O. C.; Ong, T.; Wood, D.; Yap, G. P. A.; Richeson, D. S. Transformations of Aryl Isocyanide on Guanidinate-Supported Organozirconium Complexes To Yield Terminal Imido. *Iminoacyl, and Enediamido Ligands* **2002**, *21*, 2001−2003.
(40) Martins, A. M.; Ascenso, R.; Azevedo, C. G. De.; Dias, A. R.; Duarte, M. T.; Silva, F.; Veiros, F.; Rodrigues, S. S. Insertion of Isocyanides into Group 4 Metal - Carbon and Metal - Nitrogen Bonds. In *Syntheses and DFT Calculations*, 2003; pp 4218−4228.
(41) Mcmullen, A. K.; Rothwell, I. P.; Huffman, J. C. Coupling of Acyl and Iminoacyl Groups on Zirconium and S2,p-Coordination of the Resulting Enamidolate Ligand. **1985**, 1072−1073.
(42) Bolhuis, F. Van; Boer, D.; Teuben, J. H. The Crystal Structure of a Phenyliminomethyldicyclopentadilinyltitanium(III) Complex, $Cp_2Ti\text{-}H_2\text{-}C_6H_5CN\text{-}2,6\text{-}(CH_3)_2C_6H_3$. *J. Organomet. Chem.* **1979**, *170*, 299−308.
(43) Weinert, C. S.; Fanwick, P. E.; Rothwell, I. P. Synthesis of the Tantalum Hydride Complex (R,R)-[Ta(O 2C 20H 10 {SiMe 3} 2−3,3′) 2(H)] and Reactivity with Aldehydes, Ketones, Acetylenes, and Related Substrates: A Reagent for the Asymmetric Hydrogenation of Prochiral Carbonyl Species. *Organometallics* **2005**, *24*, 5759−5766.
(44) Mulford, D. R.; Clark, J. R.; Schweiger, S. W.; Fanwick, P. E.; Rothwell, I. P. Reactions of Alkynes and Olefins with Tantalum Hydrides Containing Aryloxide Ancillary Ligation: Relevance to Catalytic Hydrogenation. *Organometallics* **1999**, *18*, 4448−4458.
(45) Semproni, S. P.; Graham, P. M.; Buschhaus, M. S. A.; Patrick, B. O.; Legzdins, P. Toward Alkane Functionalization Effected with Cp * W (NO)(Alkyl)($\eta$ 3 -Allyl) Complexes. *Organometallics* **2009**, *28*, 4480−4490.
(46) Chamberlain, L. R.; Durfee, L. D.; Fanwick, P. E.; Kobriger, L.; Latesky, S. L.; McMullen, A. K.; Rothwell, I. P.; Folting, K.; Huffman, J. C.; Streib, W. E.; Wang, R. Synthesis, structure and spectroscopic


https://doi.org/10.1021/acs.organomet.4c00338
*Organometallics* 2024, 43, 3002−3012

properties of early transition metal .eta.2-iminoacyl complexes containing aryl oxide ligation. *J. Am. Chem. Soc.* **1987**, *109*, 390−402.
(47) Nechayev, M.; Gianetti, T. L.; Bergman, R. G.; Arnold, J. C-F Sp2 Bond Functionalization Mediated by Niobium Complexes. *Dalt. Trans.* **2015**, *44*, 19494−19500.
(48) Kriegel, B. M.; Bergman, R. G.; Arnold, J. Nitrene Metathesis and Catalytic Nitrene Transfer Promoted by Niobium Bis(Imido) Complexes. *J. Am. Chem. Soc.* **2016**, *138*, 52−55.
(49) Yoshida, T.; Hirotsu, K.; Higuchi, T.; Otsuka, S. Preparation of Homoleptic T-Butyl Isocyanide Complex of Mo(0) and Reactions with Alkyl Halides. Molecular Structure of $[Mo(t\text{-}BuN = CCH_2Ph)(t\text{-}BuNC)_5]Br$. *Chem. Lett.* **1982**, *11*, 1017−1020.
(50) Wicker, B. F.; Scott, J.; Fout, A. R.; Pink, M.; Mindiola, D. J. Atom-Economical Route to Substituted Pyridines via a Scandium Imide. *Organometallics* **2011**, *30*, 2453−2456.
(51) Vicente, J.; Saura-Llamas, I.; Grünwald, C.; Alcaraz, C.; Jones, P. G.; Bautista, D. Palladium-Assisted Formation of Carbon-Carbon Bonds. Part 10. Insertion Reactions of Isocyanides into the Pd-C Bond of Orthopalladated Primary Amines. Synthesis of 2-R-Aminoisoindolinium Salts (R = TBu, 2,6-Xylyl). *Organometallics* **2002**, *21*, 3587−3595.
(52) Vicente, J.; Abad, J. A.; Martínez-Viviente, E.; Jones, P. G. Study of the Reactivity of 2-Acetyl-2-Cyano-2-Formyl-and 2-Vinyl-phenyl Palladium(II) Complexes. Mono- and Triinsertion of an Isocyanide into the Pd-C Bond. A 2-Cyanophenyl Palladium Complex as a Ligand. *Organometallics* **2002**, *21*, 4454−4467.
(53) Jordan, A. J.; Wyss, C. M.; Bacsa, J.; Sadighi, J. P. Synthesis and Reactivity of New Copper(I) Hydride Dimers. *Organometallics* **2016**, *35*, 613−616.
(54) Emerich, B. M.; Moore, C. E.; Fox, B. J.; Rheingold, A. L.; Figueroa, J. S. Protecting-Group-Free Access to a Three-Coordinate Nickel(0) Tris-Isocyanide. *Organometallics* **2011**, *30*, 2598−2608.
(55) Cardaci, G.; Bellachioma, G.; Zanazzi, P. Isocyanide Insertion Reaction in Alkylcomplexes of Iron: A Dihaptoiminoacyl Derivative of Iron(II). *Polyhedron* **1983**, *2*, 967−968.
(56) Amii, H.; Kageyama, K.; Kishikawa, Y.; Hosokawa, T.; Morioka, R.; Katagiri, T.; Uneyama, K. Preparation, Structure, and Reactions of Trifluoroacetimidoyl Palladium(II) Complexes. *Organometallics* **2012**, *31*, 1281−1286.
(57) Fandos, R.; Otero, A.; Rodríguez, A. M.; Suizo, S. Monocyclopentadienyl Titanium Complexes Supported by Functionalized Shiff Base Ligands. *J. Organomet. Chem.* **2014**, *759*, 74−82.
(58) Addison, A. W.; Rao, T. N.; Reedijk, J.; van Rijn, J.; Verschoor, G. C. Synthesis, Structure, and Spectroscopic Properties of Copper(II) Compounds Containing Nitrogen-Sulphur Donor Ligands: The Crystal and Molecular Structure of Aqua[1,7-Bis(N-Methylbenzimidazol-2'-Yl)-2,6-Dithiaheptane]Copper(II) Perchlorate. *J. Chem. Soc. Dalt. Trans.* **1984**, 1349−1356.
(59) Frisch, M. J.; Trucks, G. W.; Schlegel, H. B.; Scuseria, G. E.; Robb, M. a.; Cheeseman, J. R.; Scalmani, G.; Barone, V.; Petersson, G. a.; Nakatsuji, H.; Li, X.; Caricato, M.; Marenich, a. V.; Bloino, J.; Janesko, B. G.; Gomperts, R.; Mennucci, B.; Hratchian, H. P.; Ortiz, J. V.; Izmaylov, a. F.; Sonnenberg, J. L.; Williams; Ding, F.; Lipparini, F.; Egidi, F.; Goings, J.; Peng, B.; Petrone, A.; Henderson, T.; Ranasinghe, D.; Zakrzewski, V. G.; Gao, J.; Rega, N.; Zheng, G.; Liang, W.; Hada, M.; Ehara, M.; Toyota, K.; Fukuda, R.; Hasegawa, J.; Ishida, M.; Nakajima, T.; Honda, Y.; Kitao, O.; Nakai, H.; Vreven, T.; Throssell, K.; Montgomery, Jr. J. a.; Peralta, J. E.; Ogliaro, F.; Bearpark, M. J.; Heyd, J. J.; Brothers, E. N.; Kudin, K. N.; Staroverov, V. N.; Keith, T. a.; Kobayashi, R.; Normand, J.; Raghavachari, K.; Rendell, a. P.; Burant, J. C.; Iyengar, S. S.; Tomasi, J.; Cossi, M.; Millam, J. M.; Klene, M.; Adamo, C.; Cammi, R.; Ochterski, J. W.; Martin, R. L.; Morokuma, K.; Farkas, O.; Foresman, J. B.; Fox, D. J. G16_C01 *Gaussian 16, Revision C.01*. p ; Gaussian, Inc.: Wallin, 2016.
(60) Rassolov, V. A.; Ratner, M. A.; Pople, J. A.; Redfern, P. C.; Curtiss, L. A. 6-31G* Basis Set for Third-Row Atoms. *J. Comput. Chem.* **2001**, *22*, 976−984.
(61) Rassolov, V. A.; Pople, J. A.; Ratner, M. A.; Windus, T. L. 6-31G* Basis Set for Atoms K through Zn. *J. Chem. Phys.* **1998**, *109*, 1223−1229.
(62) Dolg, M.; Stoll, H.; Preuss, H.; Pitzer, R. M. Relativistic and Correlation Effects for Element 105 (Hahnium, Ha). A Comparative Study of M and MO (M = Nb, Ta, Ha) Using Energy-Adjusted Ab Initio Pseudopotentials. *J. Phys. Chem.* **1993**, *97*, 5852−5859.
(63) Andrae, D.; Häußermann, U.; Dolg, M.; Stoll, H.; Preuß, H. Energy-Adjusted Ab Initio Pseudopotentials for the Second and Third Row Transition Elements. *Theor. Chim. Acta* **1990**, *77*, 123−141.
(64) Kaupp, M.; Schleyer, P. V. R.; Stoll, H.; Preuss, H. Pseudopotential Approaches to Ca, Sr, and Ba Hydrides. Why Are Some Alkaline Earth MX2 Compounds Bent? *J. Chem. Phys.* **1991**, *94*, 1360−1366.
(65) Ehlers, A. W.; Böhme, M.; Dapprich, S.; Gobbi, A.; Höllwarth, A.; Jonas, V.; Köhler, K. F.; Stegmann, R.; Veldkamp, A.; Frenking, G. A Set of F-Polarization Functions for Pseudo-Potential Basis Sets of the Transition Metals ScCu, YAg and LaAu. *Chem. Phys. Lett.* **1993**, *208*, 111−114.
(66) Austin, A.; Petersson, G. A.; Frisch, M. J.; Dobek, F. J.; Scalmani, G.; Throssell, K. A Density Functional with Spherical Atom Dispersion Terms. *J. Chem. Theory Comput.* **2012**, *8*, 4989−5007.
(67) Francl, M. M.; Pietro, W. J.; Hehre, W. J.; Binkley, J. S.; Gordon, M. S.; DeFrees, D. J.; Pople, J. A. Self-Consistent Molecular Orbital Methods. XXIII. A Polarization-Type Basis Set for Second-Row Elements. *J. Chem. Phys.* **1982**, *77*, 3654−3665.
(68) Cancès, E.; Mennucci, B.; Tomasi, J. A New Integral Equation Formalism for the Polarizable Continuum Model: Theoretical Background and Applications to Isotropic and Anisotropic Dielectrics. *J. Chem. Phys.* **1997**, *107*, 3032−3041.
(69) Mennucci, B.; Tomasi, J. Continuum Solvation Models: A New Approach to the Problem of Solute's Charge Distribution and Cavity Boundaries. *J. Chem. Phys.* **1997**, *106*, 5151−5158.




https://doi.org/10.1021/acs.organomet.4c00338
*Organometallics* 2024, 43, 3002−3012